

# Transient Nucleation near the Mean-Field Spinodal

A. O. Schweiger,\* K. Barros, and W. Klein

Center for Computational Science and Department of Physics, Boston University, Boston, MA, 02215

Nucleation is considered near the pseudospinodal in a one-dimensional  $\phi^4$  model with a non-conserved order parameter and long-range interactions. For a sufficiently large system or a system with slow relaxation to metastable equilibrium, there is a non-negligible probability of nucleation occurring before reaching metastable equilibrium. This process is referred to as transient nucleation. The critical droplet is defined to be the configuration of maximum likelihood that is dynamically balanced between the metastable and stable wells. Time-dependent droplet profiles and nucleation rates are derived, and theoretical results are compared to computer simulation. The analysis reveals a distribution of nucleation times with a distinct peak characteristic of a nonstationary nucleation rate. Under the quench conditions employed, transient critical droplets are more compact than the droplets found in metastable equilibrium simulations and theoretical predictions.

PACS numbers: 05.70.Ln; 64.60.Qb; 82.20.Db

## I. INTRODUCTION

Standard nucleation theory predicts a single metastable equilibrium nucleation rate, which gives rise to an exponential distribution of nucleation times. A key assumption in the application of the standard theory is that the system is in metastable equilibrium. In practice, any system that has undergone a quench relaxes into metastable equilibrium. During this relaxation, the system has a finite probability of initiating a decay to the stable phase via an isolated droplet. This process, referred to as transient nucleation, is of both practical and theoretical interest. Experimentally, transient nucleation has been observed in the laser melting of thin silicon films [1], crystallization in amorphous alloys [2, 3], and liquid crystals [4]. Theoretical work has concentrated on mean-field kinetic descriptions [5, 6, 7, 8, 9, 10, 11, 12]. Studies of transient nucleation in  $\phi^4$  models [13, 14, 15, 16] have shown a distribution of nucleation times with a distinct peak and exponential tail.

In a mean-field system, the spinodal defines the limit of metastability. The spinodal divides the phase-diagram into two regions, one region exhibits a metastable phase while the other does not. In a system with finite but long-range interactions, the analogous limit of metastability is defined by the pseudospinodal. As the interaction range increases, statistics at the pseudospinodal converge to the corresponding mean-field spinodal values. As the pseudospinodal is approached, the metastable system exhibits diverging susceptibility, correlation length, and correlation times that are characteristic of a critical point [17, 18]. Nucleation near a pseudospinodal is structurally different from classical nucleation near the coexistence curve. In classical nucleation, droplets are compact fluctuations of the stable phase with a sharp interface separating the interior and exterior [19]. How-

ever, near the pseudospinodal, droplets do not exhibit a well-defined interface nor a stable-phase interior [20]. Evidence for nucleation near the pseudospinodal is observed in deeply quenched liquids [21, 22] and in solid-solid phase transitions [23, 24]. Our objective is to study transient nucleation rates and transient critical-droplet profiles in a system with long-range interactions near the pseudospinodal.

To make these ideas precise, we consider purely dissipative dynamics described by a Markovian Langevin equation that is a sum of a deterministic drift term and a stochastic noise term with zero mean. We define the metastable well to be the set of configurations that would follow the (noiseless) deterministic drift to a stationary configuration that is not the global energy minimum. The metastable well boundary  $\mathfrak{B}$  consists of configurations that, upon random perturbation, would each drift to the metastable minimum with probability 1/2. A similar definition is employed by Roy et al. and others [25, 26, 27]. Transient critical droplets are characterized by the most probable configuration on the metastable well boundary at a given time  $t$  since the quench.

We define the *nucleation time* as the latest time after the quench such that the system configuration was located on the metastable well boundary; the *nucleating droplet* is the corresponding system configuration. A system has nucleated when there is a negligible probability of returning to the metastable well.

Because the nucleation rate is an extensive quantity, transience is best observed when the relaxation to metastable equilibrium is slow and the system size is large. Our primary results are that in magnetic field quenches at a temperature below the critical temperature, the transient nucleation rate is adequately described by a quasi-equilibrium theory. Near the pseudospinodal, transient droplets are more compact than those that nucleate in metastable equilibrium.

In Sec. II, we introduce the model and review the field theoretic treatment of nucleation near the mean-field spinodal, the basis for the subsequent analy-

---

\*Electronic address: aschweig@physics.bu.edu

sis. Section III considers the time-dependent likelihood of non-equilibrium states characterizing relaxation to metastable equilibrium. In Sec. IV, we find the time-dependent nucleation rate and transient critical droplet as a perturbation about the metastable equilibrium critical droplet. In Sec. V, we compare our theoretical treatment to results from computer simulation. Section VI interprets and compares our results to previous work.

## II. METASTABILITY NEAR THE MEAN-FIELD SPINODAL

We consider a one-dimensional ferromagnetic system with long-range interactions prepared in equilibrium with an initially negative external field,  $h_{\text{initial}} < 0$ . At time  $t = 0$ , the system is quenched and the external magnetic field  $h$  is set to a positive value. The system then evolves toward metastable equilibrium. At some point after the quench, it will decay to the stable phase via nucleation.

The potential of the system is given by

$$V(\phi) = \epsilon\phi^2 + u\phi^4 - h\phi, \quad (1)$$

where  $\epsilon < 0$  and  $u > 0$ . For systems of interaction range  $R$ , the Ginzburg-Landau-Wilson Hamiltonian is

$$H[\phi] = \int dx \left[ \frac{R^2}{2} \left( \frac{d\phi}{dx} \right)^2 + V(\phi(x)) \right]. \quad (2)$$

We assume purely dissipative dynamics, given by the time-dependent Ginzburg-Landau equation,

$$\frac{\partial\phi}{\partial t} = -\frac{\delta H}{\delta\phi} + \eta = R^2 \frac{\partial^2\phi}{\partial x^2} - 2\epsilon\phi - 4u\phi^3 + h + \eta, \quad (3)$$

where  $\eta = \eta(x, t)$  is a zero-mean white noise with  $\langle \eta(x, t)\eta(x', t') \rangle = 2\beta^{-1}\delta(x - x')\delta(t - t')$ , and  $\beta$  is the inverse temperature. The mean-field metastable well vanishes when the applied magnetic field is the spinodal field, defined by  $h_{\text{sp}}^2 = 8|\epsilon|^3/27u$ . The corresponding mean-field spinodal magnetization satisfies  $\phi_{\text{sp}}^2 = |\epsilon|/6u$ . These quantities are obtained from setting  $dV/d\phi = d^2V/d\phi^2 = 0$ .

Under the given quench conditions, the spinodal field is positive,  $h_{\text{sp}} \gtrsim h > 0$ , and the mean-field spinodal magnetization is negative,  $\phi_{\text{sp}} < 0$ . For convenience, we introduce  $\Delta_h = h_{\text{sp}} - h$ , a measure of the depth of the metastable well.

We expand the potential about the spinodal magnetization,  $\phi_{\text{sp}}$ , retaining terms up to third order [20, 28],

$$V = \phi_{\text{sp}} \left( \Delta_h - \frac{3}{8}h_{\text{sp}} \right) + \Delta_h(\phi - \phi_{\text{sp}}) - \frac{1}{2} \frac{h_{\text{sp}}}{\phi_{\text{sp}}^2} (\phi - \phi_{\text{sp}})^3 + O((\phi - \phi_{\text{sp}})^4). \quad (4)$$

We concentrate on nucleation in the neighborhood of the metastable well. Near the spinodal, the details of the potential for large positive magnetizations has a negligible

effect on nucleation. Therefore we drop the quartic term in the subsequent analysis. Within this cubic approximation, the location of the potential minimum is

$$\phi_{\text{min}} = \phi_{\text{sp}} \left[ 1 + \sqrt{\frac{2\Delta_h}{3h_{\text{sp}}}} \right] < 0. \quad (5)$$

We introduce the shifted field,  $\psi(x) = \phi(x) - \phi_{\text{min}}$ , so that the minimum of the mean-field potential occurs precisely at  $\psi = 0$ . We rewrite the truncated potential in terms of the shifted field and drop an overall constant to obtain

$$V(\psi) = -\frac{\sqrt{6h_{\text{sp}}\Delta_h}}{2\phi_{\text{sp}}} \psi^2 - \frac{1}{2} \frac{h_{\text{sp}}}{\phi_{\text{sp}}^2} \psi^3 = a\psi^2 - b\psi^3, \quad (6)$$

where the variables  $a = -\sqrt{6h_{\text{sp}}\Delta_h}/2\phi_{\text{sp}} > 0$  and  $b = a^2/3\Delta_h > 0$  are introduced to simplify the notation. Near the mean-field spinodal, the evolution of the field in the neighborhood of the metastable well is given by a Langevin equation,

$$\frac{\partial\psi}{\partial t} = R^2 \frac{\partial^2\psi}{\partial x^2} - 2a\psi + 3b\psi^2 + \eta. \quad (7)$$

We define the stationary configurations by setting the time derivative and the noise term to zero,

$$0 = R^2 \frac{d^2\psi}{dx^2} - 2a\psi + 3b\psi^2. \quad (8)$$

Equation (8) has two spatially uniform solutions, the stable configuration,  $\psi_{\text{min}}(x) = 0$ , and an unstable configuration. There exists another non-uniform stationary configuration  $\psi_S(x)$  that corresponds to the profile of the critical droplet in metastable equilibrium [19, 20]. Because the droplet can appear anywhere in the system, we fix the center of the droplet at the origin. A droplet must be symmetric,  $\psi_S(x) = \psi_S(-x)$ , and cannot exhibit a sharp peak at its center,  $\psi'_S(0) = 0$ . At large distances, the droplet profile approaches the metastable background,  $\lim_{x \rightarrow \pm\infty} \psi_S(x) = 0$ . Solving Eq. (8), the non-uniform solution is

$$\psi_S = \frac{a}{b} \cosh^{-2} \left( x \sqrt{\frac{a}{2R^2}} \right). \quad (9)$$

This stationary configuration is unstable: assuming noiseless dynamics, a random perturbation about  $\psi_S$  would cause the system to return to its metastable well with probability 1/2. Linear stability analysis about the non-uniform solution reveals a single negative eigenvalue,  $-5a/2$ . The corresponding eigenvector gives the initial direction of growth (or decay) of the metastable equilibrium critical droplet [19, 28, 29],

$$\psi_N = \cosh^{-3} \left( x \sqrt{\frac{a}{2R^2}} \right). \quad (10)$$

The amplitude of the growth eigenvector is concentrated at its center; a spinodal critical droplet grows by first filling its center [29].

### III. CHARACTERIZING RELAXATION TO METASTABLE EQUILIBRIUM

In this section, we estimate the time-dependent likelihood of field configurations, which is required to find transient critical-droplet profiles [30, 31, 32]. After the quench, the time evolution of the probability is given by the functional Fokker-Planck equation. We sidestep the formal solution and use a quasi-static mean-field theory. We assume at a time  $t$  since the quench, the likelihood of a configuration in the metastable well can be approximated by

$$P[\psi|t] \approx C \exp \left\{ -\beta \int dx \left[ \frac{R^2}{2} \left( \frac{d\psi}{dx} \right)^2 + F_t \right] \right\}, \quad (11)$$

where  $C$  is an undetermined constant, and  $F_t = F_t(\psi)$  is a time-dependent polynomial in the field. At  $t = 0$ , Eq. (11) should agree with the equilibrium distribution prior to the quench. At long times, we must recover the metastable potential,

$$\lim_{t \rightarrow \infty} F_t = V(\psi) = a\psi^2 - b\psi^3. \quad (12)$$

Because the quench only changes the external magnetic field, we assume that  $F_t$  differs from the metastable equilibrium potential given in Eq. (6) by a time-dependent effective external field,  $J(t)$ ,

$$F_t = a\psi^2 - b\psi^3 + [h - J(t)]\psi. \quad (13)$$

In the long time limit, Eq. (12) implies that  $J(t) \rightarrow h$ . We expect that the quartic term can still be neglected since this approximation will be used when  $t$  is close to  $t_{eq}$ , when the system is in metastable equilibrium.

We choose  $J(t)$  so that the density given in Eq. (11) is consistent with the time evolution of the mean-field magnetization. In the mean-field limit, all fluctuations are suppressed and the system is described by a single scalar order parameter,  $\psi(x, t) \rightarrow m_t$ . Within the spinodal approximation, the time evolution of the mean-field system is governed by the ordinary differential equation,

$$\frac{d}{dt} m_t = -2am_t + 3bm_t^2. \quad (14)$$

The time evolution of the mean-field magnetization is,

$$m_t = \frac{2am_0}{3bm_0 + (2a - 3bm_0) \exp(2at)}, \quad (15)$$

where the initial condition  $m_0$  denotes the prequench shifted mean-field magnetization. In order that Eq. (11) reproduce the mean-field dynamics,  $F_t$  evaluated at  $m_t$  must be a minimum,

$$\left. \frac{dF_t}{d\psi} \right|_{\psi=m_t} = 0. \quad (16)$$

The expression for the time-dependent effective field is

$$J(t) = 2am_t - 3bm_t^2 + h. \quad (17)$$

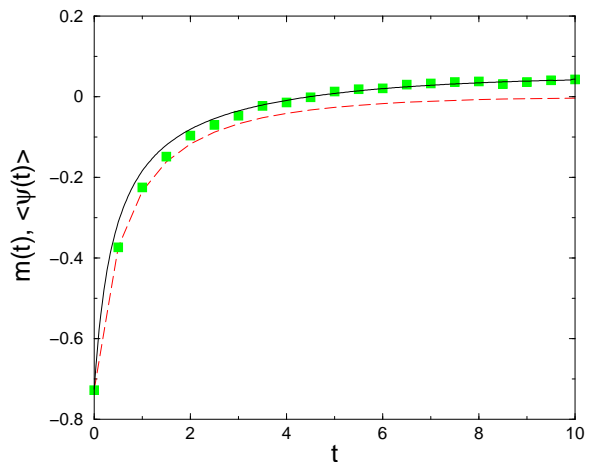


FIG. 1: The mean transient magnetization prior to nucleation (solid line) obtained from the solution of Eq. (3) compared to the average obtained from simulating Eq. (19) in metastable equilibrium (squares). Both curves rise above the metastable mean-field minimum (broken line) given by Eq. (15).

Formally, Eqs. (11), (13), and (17) define the first term of a large- $R$  asymptotic expansion of the solution to the functional Fokker-Planck equation in the metastable well near the mean-field spinodal.

Both the location of the minimum of  $F_t$  and its curvature change as a function of  $t$ . For convenience, we introduce  $\Delta_J = h_{sp} - J(t)$  and

$$A_t = \frac{1}{2} F_t''(m_t) = a\sqrt{\Delta_J/\Delta_h}, \quad (18)$$

a measure of the curvature of  $F_t$  about its minimum. At long times, the mean-field magnetization approaches its metastable equilibrium value,  $m_t \rightarrow 0$ , which implies that  $A_t \rightarrow a$  in the same limit.

For a fixed time  $t$ , we define a corresponding fictitious Langevin equation,

$$\frac{\partial \psi(x, s)}{\partial s} = R^2 \frac{\partial^2 \psi}{\partial x^2} - F_t'(\psi) + \eta(x, s), \quad (19)$$

where the coordinate  $s$  is distinct from the time  $t$  since the quench. Once in metastable equilibrium, Eq. (19) samples states from Eq. (11). We note that the states sampled by Eq. (19) must be restricted to those within the metastable well of the complete dynamics of Eq. (3). For example, configurations that would nucleate Eq. (19) must be discarded because they are not in the metastable well of the underlying dynamics. With this restriction, we use Eq. (19) to compare the statistics of Eq. (11) at a fixed time  $t$  to those generated from simulation of the complete dynamics in Eq. (3). Figure 1 compares the ensemble-averaged transient magnetization obtained from Eq. (3) to the metastable equilibrium magnetization sampled using Eq. (19) for various  $t$ .

To analytically estimate the transient magnetization of Eq. (11), we compute the stationary spatial average of

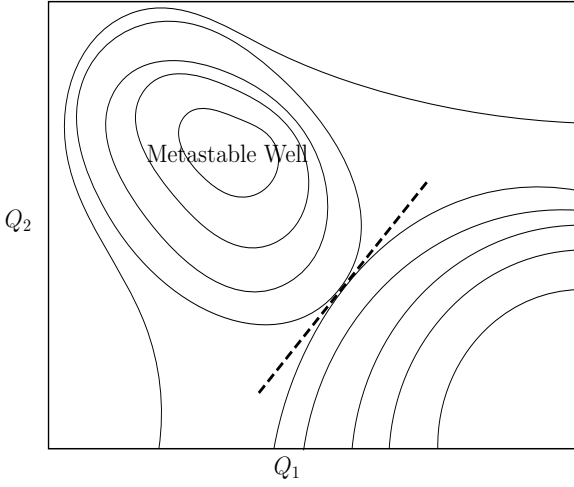


FIG. 2: Schematic equipotential curves for a model system with two arbitrary dynamical variables,  $Q_1$  and  $Q_2$ . The broken line illustrates the linearization of the metastable well boundary.

Eq. (19),

$$0 = -2a\langle\psi\rangle + 3b\langle\psi^2\rangle + J(t) - h, \quad (20)$$

which relates the first and second moments. The second moment can be approximated by the second moment of the Gaussian theory obtained by setting  $b = 0$ ,

$$\langle\psi^2\rangle \approx m_t^2 + \frac{1}{2\beta R (2A_t)^{1/2}}. \quad (21)$$

Equations (20) and (21) yield an estimate of the magnetization as a function of  $A_t$ , defined in Eq. (18),

$$\langle\psi\rangle \approx m_t + G_t^{-1} > m_t, \quad (22)$$

where,

$$G_t = 4\beta R \Delta_h a^{-1} \sqrt{2A_t} \geq G_\infty. \quad (23)$$

This estimate of the magnetization also agrees with the average magnetization obtained from simulation, shown in Fig. 1.

#### IV. TRANSIENT NUCLEATION

At a time  $t$  after the quench, the transient critical droplet  $\psi_C(x, t)$  is determined by maximizing the probability functional in Eq. (11) constrained to the metastable well boundary  $\mathfrak{B}$ ,

$$\psi_C(x, t) = \max_{\psi \in \mathfrak{B}} P[\psi|t]. \quad (24)$$

Note that the dynamically defined stationary configuration  $\psi_S$  given in Eq. (9) lies on the boundary. Furthermore, we assume that our transient critical droplets

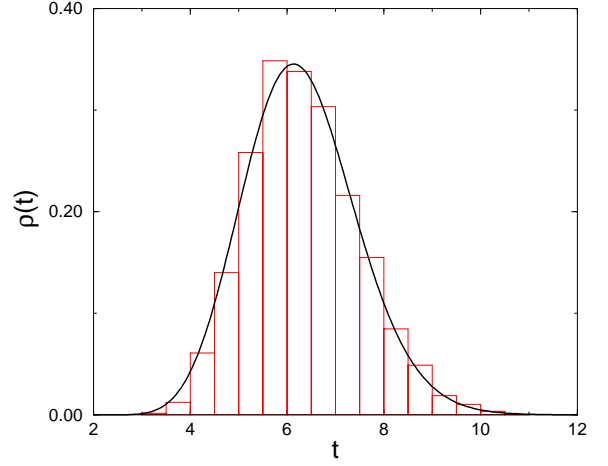


FIG. 3: The theoretical distribution of nucleation times computed from Eq. (35) (solid line) compared to the normalized histogram of nucleation times obtained from direct simulation of Eq. (3).

resemble the dynamical fixed point,  $\psi_S$ . In this limit, we approximate the metastable well boundary by a hyperplane [25] that is normal to the growth eigenvector  $\psi_N$ , given in Eq. (10). Figure 2 gives a schematic of the approximation for a two-dimensional system. Within this approximation, a boundary configuration  $\psi_{\mathfrak{B}}$  satisfies

$$\int dx (\psi_{\mathfrak{B}} - \psi_S) \psi_N = 0. \quad (25)$$

To find the configuration of maximum likelihood that satisfies the constraint, we introduce the Lagrange multiplier  $\lambda_t$  and extremize the functional,

$$\int dx \left[ \frac{R^2}{2} \left( \frac{d\psi}{dx} \right)^2 + F_t(\psi) - \lambda_t \psi \psi_N \right]. \quad (26)$$

Centered at zero, the time-dependent critical-droplet profile solves the Euler-Lagrange equation,

$$R^2 \frac{d^2 \psi_C}{dx^2} = 2a\psi_C - 3b\psi_C - J(t) + h - \lambda_t \psi_N, \quad (27)$$

where  $\lambda_t$  is chosen so that  $\psi_C$  satisfies the constraint in Eq. (25). For large  $t$ , the transient solution reduces to the dynamical fixed point,  $\lim_{t \rightarrow \infty} \psi_C = \psi_S$ . At earlier times, the equation and constraint can be solved numerically. Because we have assumed the transient critical droplet resembles the fixed point, we expect  $\lambda_t \ll 1$ . This suggests a solution as a perturbation in  $\lambda_t$ . First, we take  $\lambda_t = 0$  and find the analog to Eq. (9),

$$\psi_C^0(x, t) = m_t + \frac{A_t}{b} \cosh^{-2} \left( x \sqrt{\frac{A_t}{2R^2}} \right). \quad (28)$$

Generally, the perturbation series is

$$\psi_C(x, t) = \psi_C^0(x, t) - \lambda_t y(x, t) + O(\lambda_t^2). \quad (29)$$

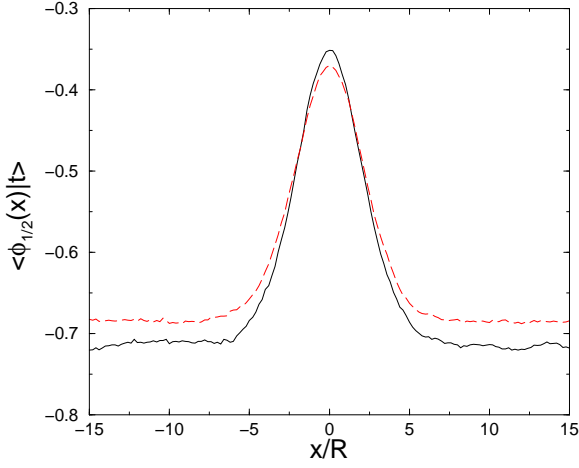


FIG. 4: Ensemble-averaged nucleating-droplet magnetization profiles from simulation at  $t = 4.5$  (solid line) and  $t = 7.5$  (broken line).

The resulting differential equation for  $y(x)$  is

$$R^2 \frac{d^2 y}{dx^2} = 2 y(x) A_t [1 - 3 \cosh^{-2}(x \sqrt{A_t/2R^2})] + \cosh^{-3}(x \sqrt{a/2R^2}). \quad (30)$$

We retain terms to first order in  $\lambda_t$ , and substitute Eq. (29) into the constraint to find the following equation for the multiplier  $\lambda_t$ ,

$$\lambda_t = \frac{\int dx (\psi_C^0(x, t) - \psi_S) \psi_N}{\int dx y(x) \psi_N}. \quad (31)$$

The effect of the constraint is to decrease the amplitude of the transient critical droplet.

With the transient droplet profiles characterized, we estimate the time-dependent nucleation rate. Given a time  $t$  before any nucleation event, there is unit probability of being in the metastable well. With this normalization, the nucleation rate is proportional to the probability to realize the transient critical droplet. We approximate this normalized probability by the relative likelihood of the transient critical droplet over the most likely metastable configuration, the uniform field with magnetization  $m_t$ ,

$$\Gamma(t) \sim \frac{P[\psi_C(x, t) | t]}{P[\psi = m_t | t]} \quad (32)$$

This rate estimate is simplified by defining the shifted effective potential,

$$\begin{aligned} \Delta F_t(\psi) &= F_t(\psi) - F_t(m_t) \\ &= A_t(\psi - m_t)^2 - 3b(\psi - m_t)^3. \end{aligned} \quad (33)$$

With this definition, the transient nucleation rate is,

$$\Gamma_t = \Gamma_0 \exp \left\{ -\beta \int dx \left[ \frac{R^2}{2} \left( \frac{d\psi}{dx} \right)^2 + \Delta F_t \right] \right\}, \quad (34)$$

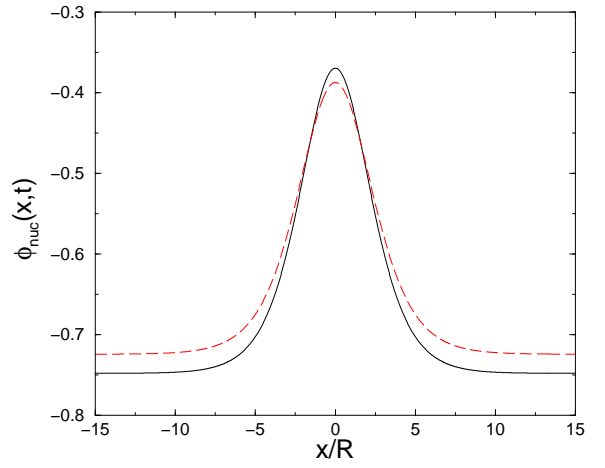


FIG. 5: Theoretical critical-droplet magnetization profiles from Eq. (29) computed at  $t = 4.5$  (solid line) and  $t = 7.5$  (broken line).

where  $\Gamma_0$  is a prefactor that depends on the details of the system [33]. For the quench considered here,  $\Gamma(t)$  is a strictly increasing function of time. The experimentally accessible nucleation time distribution is given by

$$\rho(t) = \Gamma(t) \exp \left\{ - \int_0^t dt \Gamma(t) \right\}. \quad (35)$$

## V. NUMERICAL CALCULATIONS

We simulated Eq. (3) for a periodic system of length  $L = 10^4$  where  $\epsilon = -5/9$ ,  $u = 1/4$ ,  $R = 10$ , and  $\beta = 10$ . Prior to the quench, the system is prepared in equilibrium with an external field  $h_{\text{initial}} = -1.40$  and shifted magnetization  $m_0 = -0.727$ . After the quench, the applied field is set to  $h = 0.430$ . The distance to the mean-field spinodal is  $\Delta_h = 0.021$ , and the location of the metastable minimum is given by  $\phi_{\text{min}} = -0.715$ . The corresponding parameters in the cubic approximation are  $a = 0.195$  and  $b = 0.609$ .

Throughout the run, the configuration of the system is saved periodically. Once the system has nucleated, we search for the nucleating droplet and nucleation time. We load a saved configuration and find the latest configuration that, upon perturbation, drifts to the stable phase with probability 1/2 [26]. We do not consider runs where multiple droplets appear at the nucleation time. The nucleation times were binned and compared to the theoretical results (see Fig. 3) where the free parameter  $\Gamma_0$  was chosen to produce the best fit. Ensemble-averaged nucleating droplet profiles for two different times are plotted in Fig. 4. The corresponding theoretical critical droplets obtained from Eq. (29) are plotted in Fig. 5.

Figures 4 and 5 differ slightly because they represent different statistical quantities. The cubic term in Eq. (11) give rise to a skew in the distribution. Conse-

quently, average and extremal quantities do not agree. The same effect is demonstrated in Fig. 1 and Eq. (22), where the transient system magnetization is found to differ from the mean-field magnetization. For distributions that are sufficiently peaked, we expect the discrepancies to vanish [19, 20]. This occurs when the metastable-equilibrium Ginzburg parameter  $G_\infty$  given in Eq. (23) is large. In the case considered here, the Ginzburg parameter is finite,  $G_\infty = 26$ , resulting in the contrast between the averaged configurations and the extremal configurations. However, a large  $G_\infty$  suppresses the nucleation rate,  $\Gamma \sim L \exp(-G_\infty)$ , and obscures transience in the nucleating droplets. To preserve the transient-nucleation regime while increasing the Ginzburg parameter, the system size  $L$  must scale exponentially with  $G_\infty$ .

## VI. SUMMARY AND DISCUSSION

We considered transient nucleation in a long-range one-dimensional  $\phi^4$  model with dissipative dynamics. We defined the metastable well boundary as the set of configurations balanced between the metastable and stable phases. We estimated the time-dependent likelihood of system configurations. We defined the transient critical droplet as the most likely configuration constrained to lie on the metastable well boundary. We computed the likelihood of the transient critical droplet at various times. Our results explain the nonstationarity of nucleation rates reported in studies of the time-dependent Ginzburg Landau equation.

As presented here, the theory is applicable to systems near metastable equilibrium where the system magnetization evolves slowly compared to the relaxation of other dynamical variables, as is the case near a spinodal.

The theory provides a qualitative picture of the measured ensemble-averaged profiles without any free parameters. The analysis produces a distribution of nucleation times consistent with the simulation results with a single free parameter.

Our analysis reduces to the earlier work [20] at long times, when the system has relaxed to metastable equilibrium. We found that transient droplets decay to the background magnetization in the system at the time of nucleation. Before metastable equilibrium, the background magnetization acts as an anchor: transient droplets must have greater amplitude, which in turn suppresses their rate of formation. Furthermore, this suggests that in comparable experiments, transient effects result in configurations that are more compact than predicted by the metastable equilibrium analysis. Moreover, in systems with a stable crystalline phase, these results imply transience may determine the symmetry of critical droplets when nucleating near a spinodal.

## VII. ACKNOWLEDGMENTS

We thank H. Wang whose numerical work prompted this study, A. Santos for his insightful discussions, and V. Sood and H. Gould for their careful reading of the manuscript. We also acknowledge the support of DOE grant DE-FG02-95ER14498.

- 
- [1] S. R. Stiffler, M. O. Thompson, and P. S. Peercy, "Transient nucleation following pulsed-laser melting of thin silicon films," *Phys. Rev. B* **43**, 9851 (1991).
  - [2] H. Kumomi and T. Yonehara, "Transient nucleation and manipulation of nucleation sites in solid-state crystallization of a-Si films," *J. Appl. Phys.* **75**, 2884 (1994).
  - [3] Y. X. Zhuang, J. Z. Jiang, Z. G. Lin, M. Mezouar, W. Crichton, and A. Inoue, "Evidence of eutectic crystallization and transient nucleation in  $\text{Al}_{89}\text{La}_6\text{Ni}_5$  amorphous alloy," *Appl. Phys. Lett.* **79**, 743 (2001).
  - [4] V. Sergan, Y. Reznikov, J. Anderson, P. Watson, J. Ruth, and P. Bos, "Mechanism of relaxation from electric field induced homeotropic to planar texture in cholesteric liquid crystals," *Mol. Cryst. Liq. Cryst.* **330**, 1339 (1999).
  - [5] Ya. B. Zeldovich, *Acta Physicochim. URSS* **18**, 1 (1943).
  - [6] K. F. Kelton, A. L. Greer, and C. V. Thompson, "Transient nucleation in condensed systems," *J. Chem. Phys.* **79**, 6261 (1983).
  - [7] V. A. Shneidman, "Transient critical flux in nucleation theory," *Phys. Rev. A* **44**, 2609 (1991).
  - [8] D. T. Wu, "The time lag in nucleation theory," *J. Chem. Phys.* **97**, 2644 (1992).
  - [9] B. E. Wyslouzil and G. Wilemski, "Binary nucleation kinetics. III. Transient behavior and time lags," *J. Chem. Phys.* **105**, 1090 (1996).
  - [10] I. L. Maksimov, M. Sanada, and K. Nishioka, "Energy barrier effect on transient nucleation kinetics: Nucleation flux and lag-time calculation," *J. Chem. Phys.* **113**, 3323 (2000).
  - [11] L. S. Bartell and G. W. Turner, "Transient Nucleation: Computer Simulation vs Theoretical Inference," *J. Phys. Chem. B* **108**, 19742 (2004).
  - [12] D. Kashchiev, "Moments of the rate of nonstationary nucleation," *J. Chem. Phys.* **122**, 114506 (2005).
  - [13] D. Boyanovsky, R. Holman, D. S. Lee, and J. P. Silva, "A Note on Thermal Activation," *Nucl. Phys. B* **441**, 595 (1995).
  - [14] S. Seunarine and D. McKay, "Additive and multiplicative noise driven systems in 1+1 dimensions: Waiting time extraction of nucleation rates," *Phys. Rev. D* **64**, 105015 (2001).
  - [15] M. Gleiser, R. C. Howell, "Resonant Nucleation," *Phys. Rev. Lett.* **94**, 151601 (2005).
  - [16] H. Wang, K. Barros, A. Schweiger, H. Gould, and W. Klein, in preparation.
  - [17] N. Gulbahce, H. Gould, and W. Klein, "Zeros of the partition function and pseudospinodals in long-range Ising models," *Phys. Rev. E* **69**, 036119 (2004).
  - [18] M. A. Novotny, W. Klein, P. A. Rikvold, "Spinodals and transfer matrices in d=1 models," *Phys. Rev. B* **33**, 7729 (1986).

- (1986).
- [19] J. S. Langer, “Theory of the condensation point,” *Ann. Phys.* **41**, 108 (1967).
  - [20] C. Unger and W. Klein, “Nucleation theory near the classical spinodal,” *Phys. Rev. B* **29**, 2698 (1984).
  - [21] J. X. Yang, H. Gould, W. Klein, “Molecular-Dynamics Investigation of Deeply Quenched Liquids,” *Phys. Rev. Lett.* **60**, 2665 (1988).
  - [22] F. Trudu, D. Donadio, and M. Parrinello, “Freezing of a Lennard-Jones Fluid: From Nucleation to Spinodal Regime,” *Phys. Rev. Lett.* **97**, 105701 (2006).
  - [23] F. J. Cherne, M. I. Baskes, R. B. Schwarz, S. G. Srinivasan, and W. Klein, “Non-classical nucleation in supercooled nickel,” *Model. Simul. Mater. Sci. Eng.* **12**, 1063 (2004).
  - [24] C. J. Gagne, H. Gould, W. Klein, T. Lookman, and A. Saxena, “Simulations of Spinodal Nucleation in Systems with Elastic Interactions,” *Phys. Rev. Lett.* **95**, 095701 (2005).
  - [25] A. Roy, J. M. Rickman, J. D. Gunton, and K. R. Elder, “Simulation study of nucleation in a phase-field model with nonlocal interactions,” *Phys. Rev. E* **57**, 2610 (1998).
  - [26] L. Monette, W. Klein, and M. Zuckermann, “Monte Carlo study of the effect of perturbations on critical droplets,” *J. Stat. Phys.* **66**, 117 (1992).
  - [27] W. E, W. Ren, and E. Vanden-Eijnden, “Transition pathways in complex systems: Reaction coordinates, isocommittor surfaces, and transition tubes,” *Chem. Phys. Lett.* **413**, 242 (2005).
  - [28] M. Büttiker and R. Landauer, “Nucleation theory of overdamped soliton motion,” *Phys. Rev. A* **23**, 1397 (1981).
  - [29] C. Unger and W. Klein, “Initial-growth modes of nucleation droplets,” *Phys. Rev. B* **31**, 6127 (1985).
  - [30] J. S. Langer, “Statistical theory of the decay of metastable states,” *Ann. Phys.* **54**, 258 (1969).
  - [31] K. Binder, “Time-Dependent Ginzburg-Landau Theory of Nonequilibrium Relaxation,” *Phys. Rev. B* **8**, 3423 (1973).
  - [32] D. Reguera, J. M. Rubí, and A. Pérez-Madrid, “Fokker-Planck equations for nucleation processes revisited,” *Physica A* **259**, 10 (1998).
  - [33] The prefactors  $\Gamma_0$  and  $C$  in Eq. (11) implicitly depend on time. For a sufficiently compact distribution of nucleation times, both  $\Gamma_0$  and  $C$  are effectively constant.